Author

Xiongyu Chen

Title
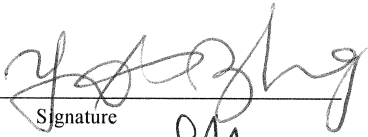
CO_2 diffusion in dry and hydrous haplobasaltic melts

submitted in partial fulfillment of the requirements for the degree of
Master of Science in Geology
Department of Earth and Environmental Sciences
The University of Michigan
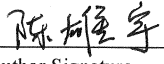
Accepted by:

Signature	Youxue Zhang	6/19/12
	Name	Date
Signature	Jie (Jackie) Li	06/19/12
	Name	Date
Department Chair Signature	Rebecca Lange	6/21/12
	Name	Date

Earth and Environmental Sciences
UNIVERSITY OF MICHIGAN

CO$_2$ diffusion in dry and hydrous haplobasaltic melts

Xiongyu Chen

Department of Earth and Environmental Sciences, University of Michigan, Ann Arbor,

Michigan 48109, USA

Email: haplobasalt@gmail.com

Abstract: Carbon dioxide diffusion kinetics plays a significant role in the degassing process of some mid-ocean-ridge basalt (MORB) and ocean island basalt (OIB). However, CO$_2$ chemical diffusion in hydrous melt is little studied. Diffusion couple experiments have been carried out to investigate total CO$_2$ diffusion in both dry and hydrous haplobasaltic melts with a bulk composition of 43 wt% Anorthite and 57 wt% Diopside, or shortly An$_{43}$Di$_{57}$. Fourier Transform Infrared (FTIR) Spectroscopy is utilized to measure CO$_2$ and H$_2$O contents and concentration profiles. The total CO$_2$ diffusion data are fit with two Arrhenius equations, one is for dry An$_{43}$Di$_{57}$ melt at 1.0 GPa and a temperature range of 1400-1594 °C (excluding one outlier point):

$$lnD(CO_{2,t}) = -2.78 - 38319/T; \ R^2 = 0.996$$

where D is in m^2/s and T is in K; the other is for hydrous An$_{43}$Di$_{57}$ melt with 2.63 wt% H$_2$O at 1.0 GPa and a temperature range of 1387-1596 °C (excluding two outlier points):

$$lnD(CO_{2,t}) = -10.75 - 21472/T; \ R^2 = 0.944$$

Key words: CO$_2$ diffusion, dry and hydrous melts, An$_{43}$Di$_{57}$, FTIR

Introduction

Carbon dioxide is the second most abundant volatile component in magmas, after H$_2$O. In basaltic melts, the partial pressure of CO$_2$ is often much higher than that of H$_2$O due to

the low solubility of CO_2. For instance, the dissolved CO_2 content in mid-ocean ridge basalt (MORB) could be as high as 360ppm (Dixon et al., 1988), equivalent to a CO_2 partial pressure of 72 MPa (Dixon et al., 1995). In contrast, H_2O content in MORB could be as high as 1.5 wt% (Dixon et al., 1988; Workman et al., 2006), equivalent to a H_2O partial pressure of 14 MPa. Since CO_2 has a higher partial pressure than H_2O in most MORB and ocean island basalt (OIB), CO_2 transport dominates the gas bubble growth in most MORB and OIB. Dixon et al. (1988) reported 13 MORB glasses at different locations, with a mean water depth of 2000m or a mean pressure of 20 MPa, have more than 200 ppm CO_2 (saturation pressure of 40 MPa). It indicates these MORBs are oversaturated with 2 times of equilibrium CO_2. Thus, the CO_2 diffusion kinetics is very important in some MORB degassing processes.

CO_2 component may be present in silicate melts as molecular CO_2 (hereafter referred as $CO_{2,m}$) and CO_3^{2-} (dissolved carbonate groups) (Fine and Stolper, 1985; Fine and Stolper, 1986). The reaction between the two species is written as:

$$CO_{2,m}(melt) + O^{2-}(melt) \Leftrightarrow CO_3^{2-}(melt) \qquad (1)$$
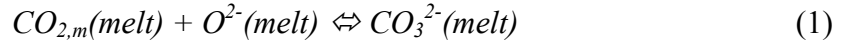
where O^{2-} is free oxygen anion, the equilibrium equation is:

$$K = \frac{a(CO_3^{2-})}{a(CO_{2,m}) \cdot a(O^{2-})} \qquad (2)$$

where K is the equilibrium constant, and $a(CO_3^{2-})$, $a(CO_{2,m})$ and $a(O^{2-})$ are the activities of CO_3^{2-}, $CO_{2,m}$ and O^{2-}, respectively.

Diffusion of CO_2 in different silicate melts has been widely studied. Watson et al. (1982) first studied dissolved carbonate diffusion in sodium aluminosilicate and haplobasaltic melts with a ^{14}C thin-source tracer technique. They discovered a remarkable phenomenon that the dry sodium aluminosilicate melt and the dry haplobasaltic melt have similar CO_2 diffusion properties. Further study by Watson et al. (1991) and Nowak et al. (2004) confirm that the bulk CO_2 diffusivity does not depend on anhydrous silicate melt

composition. To investigate H_2O effect on CO_2 diffusion in silicate melts, Watson (1991) determined ^{14}C radiotracer diffusivity in obsidian and dacite melts with 0-11 wt% H_2O at 800-1100 °C and 1 GPa. Sierralta et al. (2002) measured the bulk CO_2 diffusivity in albite melt with 0-2 wt% H_2O at 1250 °C and 0.5 GPa with the diffusion couple method, of which only three samples have 0.73, 2.0 and 2.0 wt% H_2O_t. Both study shows that ^{14}C-tracer/ CO_2 diffusivity increases exponentially with H_2O.

Zhang et al. (2007) reviewed both ^{14}C tracer diffusivity and CO_2 effective binary diffusivity in silicate melts and found they are different by a factor of 7 to 20. Mungall (2002) and Zhang and Ni (2010) attributed the difference to inaccuracy of the ^{14}C diffusion data by β-track mapping due to β particle range. In this study, the total CO_2 diffusivity will be measured.

The paucity of CO_2 diffusivity data in hydrous melt makes it necessary to carry out an experimental study of CO_2 diffusion in hydrous melt. This study is an attempt to improve CO_2 diffusion data, especially for hydrous silicate melts. The composition chosen is iron-free so that IR spectra can be measured easily. Since the CO_2 diffusivity is roughly independent of silicate melt composition, the new data is expected to be applicable to CO_2 diffusion in many other hydrous silicate melts.

Materials and experiment techniques

Starting Materials

The 5 starting glasses were synthesized in the lab of Harald Behrens at the University of Hannover, named as AnDi0, AnDi1, AnDi2, AnDi3, AnDi4 and AnDi5, where AnDi denotes composition of $An_{43}Di_{57}$. This composition may also be regarded as haplobasalt. The samples are described below.

(1) AnDi0 is the only dry and CO_2-free glass, which is synthesized by fusion of CaO, Al_2O_3, SiO_2 and MgO oxide powders at 1600 °C for 2 hours.

(2) AnDi1, AnDi2, AnDi3 and AnDi5 are hydrous and CO_2-bearing glasses, they are prepared by mixing dry CaO, Al_2O_3, SiO_2 and MgO oxide powders with different portions of silver oxalate, then loading the four powder mixtures and doubly distilled water in four gold-palladium capsules. After being sealed by welding, the four capsules are heated in an internally heated pressure vessel (IHPV) so that all water and carbon dioxide would be dissolved in under-saturated conditions. The heating conditions for AnDi1, AnDi2 and AnDi3 is 1250 °C and 5 kbar for 2 hours, 1300 °C and 3 kbar for 3 hours, and 1300 °C and 4 kbar for 2 hours, respectively. Finally the capsules are rapidly quenched to crystal-free samples.

(3) AnDi4 is the only dry and CO_2 bearing glass, it was prepared by mixing dry CaO, Al_2O_3, SiO_2 and MgO oxide powders with silver oxalate and then loading the powder mixture in a gold-palladium capsule, followed by sealing, heating and quench steps in (2). The heating condition is at 1400 °C and 4 kbar for 10 minutes. All the glasses are transparent and crystal free, but some of them contain very tiny amount of bubbles.

Fourier Transform Infrared (FTIR) Spectroscopy

   The six starting glasses are first checked for homogeneity in terms of CO_2 and H_2O contents. From each of them one thin slice was cut and doubly polished to a ~0.15 mm thin wafer. The FTIR spectra of these six wafers are acquired to determine H_2O and CO_2 contents. FTIR analyses were conducted with a Perkin Elmer Spectrum GX FTIR spectrometer attached with a microscope. The instrumental condition is KBr beamsplitter, MCT detector, IR source, 100μm × 100μm aperture size, 4.00 cm^{-1} resolution, gain of 1 and IR range of 7800-400 cm^{-1}. When analyzing total CO_2 concentration profiles, an

aperture size of 15 μm × 200 μm was chosen as a result of considering both a good spatial resolution and a good IR background energy. Along the direction of aperture's short side, also the cylinder-axis or diffusion direction, three profiles, each with about 40 points, are measured near the wafer's center to verify the horizontal homogeneity of the samples and to improve the precision of diffusivity measurements by averaging CO_2 diffusivity from three profiles.

The absorbance (A) of an IR band at certain wave number is converted to species concentrations with Beer's law (Stolper, 1982):

$$C = \frac{wA}{\varepsilon d \rho}$$ (3)

where C is the mass fraction of the species expressed on an oxide molecule basis, w is the molar mass of the oxide component (one component can have more than one species, e.g. CO_2 has CO_{2m} and CO_3^{2-}), ε is the molar absorptivity, d is the thickness, and ρ is the density. The thickness is measured with a digital indicator (uncertainty is 2 μm).

There is no available calibration for IR measurements of CO_2 and H_2O concentrations in $An_{43}Di_{57}$ glass. Hence, molar absorptivities for basaltic glasses are used for the $An_{43}Di_{57}$ glass (haplobasalt). The molar absorptivities of CO_2 species adopt from Fine and Stolper (1985 and 1986). The band at 2349 cm^{-1} is due to asymmetric stretching of molecular CO_2 ($CO_{2,m}$) and has a molar absorptivity of 945±45 L·mol^{-1}·cm^{-1}. The doublet bands at 1515 cm^{-1} and 1435 cm^{-1} are due to the anti-symmetric stretching of distorted CO_3^{2-} group and both have a molar absorptivity of 375±20 L·mol^{-1}·cm^{-1}.

Zhang (1999) reviewed the IR calibration of H_2O in silicate glasses. The molar absorptivities of H_2O species adopt from Dixon et al. (1988 and 1995). The band at 5200 cm^{-1} is due to molecular H_2O (hereafter referred as H_2O_m) bending and stretching (Scholze 1960), and has a molar absorptivity of 0.62 L·mol^{-1}·cm^{-1}. The band at 4500 cm^{-1} is due to XOH bending/stretching + OH basic stretching (Stolper, 1982) and has a molar

absorptivity of 0.67 L·mol^{-1}·cm^{-1}. The band at 3550 cm^{-1} is due to the fundamental OH

stretching (Scholze, 1959; Nakamoto, 1978) and therefore represents the total water

(hereafter referred as H$_2$O$_t$), and this band has a molar absorptivity of 63 L·mol^{-1}·cm^{-1}.

Pandya et al. (1992) and Danyushevsky et al. (1993) also calibrated the molar

absorptivity of the 3550 cm^{-1} band in basaltic glasses, which are 61 and 60.6 L·mol^{-1}·cm^{-1},

similar to Dixon et al.'s (1988 and 1995). The band at 1630 cm^{-1} is due to the

fundamental bending of dissolved molecular H$_2$O (Nakamoto, 1978) and has a molar

absorptivity of 25 L·mol^{-1}·cm^{-1}. A wide band at 2380 cm^{-1} is observed. The assignment of

this peak will be discussed later.

Electron Microprobe Analysis (EMPA)

   The major element of the six starting glasses is analyzed with a Cameca SX-100

Electron Microprobe analyzer (EMPA). The instrumental condition is a voltage of 15 KV,

a current of 10 nA, and 10 μm resolution. A low resolution is chosen because the samples

are big and homogenous in terms of bulk composition such that EMPA is used to

determine the average bulk composition of each starting glass. The EMPA has five

vertical wavelength-dispersive spectrometers (WDS), which can analyze five elements

simultaneously. The measurement of each element needs calibration with a standard

sample, although one standard could calibrate for several elements. In both FTIR and

EMPA analysis, several random points of each wafer are analyzed.

   The major oxide concentrations are listed in table 1. The composition is roughly

An$_{43}$Di$_{57}$. The glass density is calculated with the equation:

$$\rho(AnDi) = \frac{1}{w(An)/\rho(An) + w(Di)/\rho(Di)} - 0.0179 \cdot c_{water} \tag{4}$$

where ρ(An) and ρ(Di) is the room temperature density of Anorthite glass and Diopside

glass, respectively: ρ(An)=2.704 g·cm^{-3} (Taniguchi, 1989; Knoche et al., 1992) and

$\rho(Di)= 2.851$ g·cm^{-3} (Lange, 1997; Knoche et al., 1992), *w(An)* and *w(Di)* is the best fit of Anorthite weight percent and Diopside weight percent, respectively, and c_{water} is water concentration in wt%,. The density decrease per weight percent water is from the calibration of Benne and Behrens (2003), who used similar AnDi glasses.

Diffusion couple Experiment

The total CO_2 diffusivity in dry and hydrous haplobasaltic melts is measured with the diffusion couple method. The procedure is revised from Zhang et al. (1991) and a sketch of sample assemblage and capsule can be found in Ni et al. (2009). The diffusion couple consists of two doubly polished cylinders. Both cylinders have a diameter of ~2 mm, a height of ~2 mm, and very similar H_2O content but different CO_2 content. The two cylinders touch each other on one smooth surface and then together are packed snugly in a platinum capsule (for dry experiments) or a graphite capsule (for hydrous experiments). The axes of the two cylinders and the capsule are roughly parallel so that the interface is roughly horizontal. All the dry diffusion couples use AnDi4 vs. AnDi0. All the hydrous diffusion couples use AnDi1 vs. AnDi2 except the last one uses AnDi1 vs. AnDi3 since AnDi2 had been used up by then. To prevent convection, the lower cylinder is denser and with less CO_2 and H_2O. The capsule is placed in a crushable MgO sleeve and then encased in a ~32-mm-long graphite furnace and then wrapped with lead foil. The experiment is conducted in a piston-cylinder apparatus at 1390-1600 °C and 1.0 GPa, except the first experiment is done at 0.5 GPa. At each temperature and pressure, two or more experiments are done at very different durations (~a factor of 4) to check whether there is convection. If convection significantly influences CO_2 diffusion, then $CO_{2,t}$ diffusivity at the same temperature and pressure would depend on time. Otherwise, $CO_{2,t}$ diffusivity would be roughly constant within the time series. Before experiment, the

apparatus is relaxed at 200 °C and 10~15% higher than experimental pressure in order to close all the gaps (known as 'piston out' procedure). Temperature is controlled and recorded by an automatic control system connected with a Pt-Pt$_{90}$Rh$_{10}$ thermocouple. During experiment there is no temperature overshoot and the fluctuation is less than 2 °C. After the experiment runs 1-60 min, which depends on the estimated diffusivity, the power is shut off and the furnace is quenched by 10°C chilled water. After experiment, the furnace is impregnated in epoxy and then doubly polished to a 0.15 mm thin wafer, which is parallel to the cylinders' axis and near the center.

Within some of the transparent wafers, a few tiny bubbles with a diameter of about 5 μm are observed under microscope. These bubbles are probably dissolved air during the experiment. The volume of bubbles is negligible compared with the volume of two cylinders (a rough estimate of their ratio is 1:10^6), the dissolved bubbles are roughly air and their density is less than 10^{-3} of the An$_{43}$Di$_{57}$ glass density, and CO$_2$ concentration in air and that in the An$_{43}$Di$_{57}$ glasses are at the same order; hence, the bubbles observed in some of the diffusion couples contribute nothing to total CO$_2$ diffusivity.

In order to make sure the samples are molten in every experiment, the melting point of the An$_{43}$Di$_{57}$ glasses must be known. The glasses have a composition of An$_{43}$Di$_{57}$, thus have a melting point of 1417 °C (Presnall et al. 1978 reported the melting point of An$_{40}$Di$_{60}$ at 0.7 GPa and 1.0 GPa is 1391°C and 1417 °C, respectively). In dry experiments, there is only 0.04 wt% H$_2$O in the melt, whose effect on melting point is negligible. But in hydrous experiments, H$_2$O can be as high as 2.7 wt%, which significantly lowers the melting point. Using the colligative property of dilute solution, the melting point drop ΔT_f can be found with (no need to consider CO$_2$ here) :

$$\Delta T_f = \frac{R(T_f^*)^2}{\Delta_{fus}H_{m,A}^*} \bullet \frac{M_A / M_B}{m(A) / m(B)} \tag{5}$$

where R is the universal gas constant and equals 8.314 J•mol^{-1}•K^{-1}, $\Delta_{fus}H^{*}_{m,A}$ is the fusion enthalpy of An$_{43}$Di$_{57}$ and equals 135.6 kJ/mol (data from Richet et al., 1984), T_f^{*} is the melting point of dry An$_{43}$Di$_{57}$ and equals 1417 °C, M_B is the molar mass of H$_2$O and equals 18.02 g•mol^{-1}, $m(B)$ is the content of H$_2$O in the glass and equals 2.7 wt%, M_A is the molar mass of An$_{43}$Di$_{57}$ and equals 242.72 g•mol^{-1}, and $m(A)$ is the content of An$_{43}$Di$_{57}$ in the glass and equals 97.3 wt%. The calculated melting point drop is 65.7 °C and the melting point of the An$_{43}$Di$_{57}$ glass with 2.7 wt% H$_2$O is 1351 °C. Since the temperature drop from the interface to the end of a cylinder is 20~30 °C, depending on both the interface temperature and the cylinder length, the nominal interface temperature of hydrous experiment has to be higher than 1380 °C.

Results

CO$_2$ and H$_2$O contents in starting glasses

The densities and CO$_2$ and H$_2$O contents of AnDi0, AnDi1, AnDi2, AnDi3, AnDi4 and AnDi5 are listed in table 1. The total CO$_2$, hereafter referred as CO$_{2,t}$, is the sum of CO$_{2,m}$ and the average CO$_3^{2}$ calculated by 1510 cm^{-1} band and 1430 cm^{-1} band. In the hydrous glasses, there is no detectable molecular CO$_2$ and CO$_3^{2-}$ is the only CO$_2$ species. In the dry glasses, H$_2$O$_t$ is directly calculated by 3550 cm^{-1} band since only this band is detectable. In hydrous glasses, H$_2$O$_t$ is the sum of H$_2$O$_m$ calculated by 5200 cm^{-1} band and OH calculated by 4500 cm^{-1} band. The An$_{43}$Di$_{57}$ glasses are not homogeneous in terms of H$_2$O and CO$_2$ contents, which will result in some scatters in the diffusion profiles.

FTIR spectra

Figure 1 shows the background (AnDi0) subtracted spectra of AnDi1, AnDi2, AnDi3 and AnDi5. In the calibration done by Dixon et al. (1988; 1995), the 5200 cm^{-1} band and

4500 cm^{-1} band were fit together with a flat and unbiased curve line. Unlike the calibration, the 4500 cm^{-1} band baseline in the An$_{43}$Di$_{57}$ glasses has a very sharp slope at lower wavenumber side, which makes the baseline's curvature underneath 4500 cm^{-1} band very uncertain. As a result, the uncertainty of H$_2$O$_t$ can be as large as 7%. Since this study only needs an average H$_2$O$_t$ for each experiment, the less than 7% uncertainty in H$_2$O$_t$ is not a big issue.

A band at 2370 cm^{-1} is observed in all hydrous and CO$_2$ bearing glasses, such as AnDi1, AnDi2, AnDi3 and AnDi5, but is absent in the dry AnDi0 and AnDi4. This 2370 cm^{-1} band has a full width at half maximum (FWHM) of about 180 cm^{-1} and the variability of peak position is ±10 cm^{-1}. On the contrary, the CO$_{2,m}$ band at 2349 cm^{-1} is only observed in the dry and CO$_2$ bearing AnDi4. This 2349 cm^{-1} band has a FWHM of about 30 cm^{-1} and the variability of peak position is ±2 cm^{-1}. As can be seen in figure 2, the 2370 cm^{-1} band observed in AnDi3 is a very different band from the CO$_{2,m}$ band at 2349 cm^{-1} observed in AnDi4. Zarubin (1999) and Behrens et al. (2003) reported the ABC triplet of hydroxyl group at 2800 cm^{-1}, 2400 cm^{-1} and 2000-1700 cm^{-1}, respectively. Neither the A band nor the C band is observed in hydrous An$_{43}$Di$_{57}$ glasses; as a result, the 2370 cm^{-1} band cannot be readily assigned to the B band of the hydroxyl triplet.

Because the band at 2370 cm^{-1} is only observed in hydrous and CO$_2$ bearing An$_{43}$Di$_{57}$ glasses and not in dry and CO$_2$ bearing An$_{43}$Di$_{57}$ glass, so this band must be, but maybe not exclusively, related to H$_2$O. To testify whether the band at 2370 cm^{-1} is also related to CO$_{2,m}$ or just whether CO$_{2,m}$ is important in hydrous and CO$_2$ bearing glasses, an AnDi5 spectrum is subtracted from an AnDi2 spectrum at the same thickness. AnDi2 and AnDi5 have very similar H$_2$O content but very different CO$_2$ content. As it can be seen in figure 2, a very tiny peak is observed at 2349 cm^{-1}. This tiny peak could be due to molecular CO$_2$, but could also be due to small difference when subtracting one large peak from

another large peak. If it is due to molecular CO_2, the $CO_{2,m}$ content is less than 0.5% of CO_3^{2-} content, which is smaller than IR's 1% uncertainty. If it is due to a small difference in subtraction, the band at 2370 cm^{-1} is thereby not related to CO_2. Hence, in either case, in the hydrous and CO_2 bearing $An_{43}Di_{57}$ glasses, $CO_{2,m}$ is ignored and CO_3^{2-} is the only CO_2 species.

CO$_2$ diffusivity

Twelve diffusion couple experiments were carried out to investigate the total CO_2 diffusivity in both dry and hydrous $An_{43}Di_{57}$ melts. They are named as DifAnDi-101 to DifAnDi-112. DifAnDi-101 to DifAnDi-106 are dry experiments, of which DifAnDi-105 failed due to thermocouple failure. DifAnDi-107 to DifAnDi-112 are hydrous experiments. Table 2 lists the experimental conditions and diffusivity data. Figure 3 shows the $CO_{2,t}$ content profiles in all diffusion couple experiments. Before fitting the diffusivity data with the Arrhenius equations, data quality is checked below.

First, the reproducibility of diffusivity in different profiles of each single experiment is examined. Table 2 shows, of three different profiles in DifAnDi-103, DifAnDi-104 and DifAnDi-111, the two times standard deviation of diffusivity is less than 40% of the average, meaning the data quality is fine. For the other eight experiments, the two times standard deviation of diffusivity in three different profiles is less than 30% of the average, meaning the data quality is fairly good. Second, the reproducibility of diffusivity is checked by making a plot of diffusivity versus time. Figure 4 shows, at the condition of ~1460 °C, 1.0 GPa and no water, the diffusivity values of DifAnDi-103 and DifAnDi-104 are very similar but are smaller than that of DifAnDi-102 and the difference is a factor of 1.8; at the condition of ~1450 °C, 1.0 GPa and ~2.63 wt% water, the diffusivity values of DifAnDi-108 and DifAnDi-109 are similar but are smaller than that of DifAnDi-107 and

the difference is a factor of 2.1; and at the condition of ~1390 °C, 1.0 GPa and ~2.63 wt% water, the diffusivity value of DifAnDi-111 is smaller than that of DifAnDi-110 and the difference is a factor of 2.6. The diffusivity data are not well reproduced within the time series of the same temperature, pressure and water content. As a consequence, some of the dry and hydrous experiments will be excluded as outliers when fitting the Arrhenius equations. Out of the six dry experiments, one failed, and one is an outlier. Out of the six hydrous experiments, there are two outliers. The exact reason is not clear and there is no clear evidence to testify which experiment was affected by convection. Effort is still being made to clarify the issue.

The current available $CO_{2,t}$ diffusion data in dry melts at 550-1340 °C and 0.11-1 GPa have been reviewed by Zhang et al. (2007) and fit with (Equation 30 in Zhang et al., 2007):

$$lnD_{CO2,total} = -14.69 - 16915/T + 0.2056P/T$$

where P is in MPa. According to the above equation, the diffusivity at 1.0 GPa increases 1.06 in terms of lnD when temperature increases from 1400 °C to 1600 °C; while the diffusivity at 1400 °C only increases 0.07 in terms of lnD when pressure increases from 0.5 GPa to 1.0 GPa. For this reason, the pressure dependence of $CO_{2,t}$ diffusivity in dry melts is ignored and DifAnDi-101 (ran at 0.5 GPa) is fit together with other dry experiments. Fitting all the dry experiments except for one outlier, DifAnDi-102, yields the following Arrhenius equation for $CO_{2,t}$ diffusivity in dry $An_{43}Di_{57}$ melt at 1.0 GPa and a temperature range of 1400-1594 °C:

$$lnD(CO_{2,t}) = -2.78 - 38319/T; \quad R^2 = 0.996 \tag{6}$$

where the unit of $D(CO_{2,t})$ and T is m^2/s and K, respectively. The activation energy implied by Equation (6) is 318.58 kJ·mol^{-1}.

The average and 2 times standard deviation of H_2O_t content in all hydrous experiments is 2.63 wt% and 0.03 wt%, respectively. Although typically IR's relative uncertainty is roughly 1%, as discussed in the last section the relative uncertainty of H_2O_t content in $An_{43}Di_{57}$ glasses can be as large as 7%. The total water content in all hydrous experiments is roughly constant: 2.63 wt%. Fitting all the hydrous experiments except for two outliers, DifAnDi-107 and DifAnDi-110, yields the following Arrhenius equation for $CO_{2,t}$ diffusivity in hydrous $An_{43}Di_{57}$ melt with 2.63 wt% water at 1.0 GPa and a temperature range of 1387-1596 °C:

$$lnD(CO_{2,t}) = -10.75 - 21472/T; \ R^2 = 0.944 \tag{7}$$

The activation energy implied by Equation (7) is 178.52 kJ·mol^{-1}. Although the coefficients of determination of Equation (6) and (7) is nearly 1, it should be noted that it is after excluding one outlier point and two outlier points, respectively. Figure 5 is a plot of the diffusivity data of all experiments and the two best-fit lines given by Equation (6) and (7).

Discussion

Figure 5 shows the existence of water significantly increases $CO_{2,t}$ diffusivity in $An_{43}Di_{57}$ melt. The mechanism of water increasing $CO_{2,t}$ diffusivity is to make the melt less viscous. $An_{43}Di_{57}$ melt viscosity is estimated with the general viscosity equation of silicate melts (Hui et al., 2007). At 1400 °C and 1.0 GPa, the viscosity of dry $An_{43}Di_{57}$ melt and hydrous $An_{43}Di_{57}$ melt with 2.63 wt% water is 4.051 Pa·s and 3.243 Pa·s, respectively. At 1600 °C and 1.0 GPa, the viscosity of dry $An_{43}Di_{57}$ melt and hydrous $An_{43}Di_{57}$ melt with 2.63 wt% water is 0.161 Pa·s and 0.133 Pa·s, respectively. It can be seen, the decrease of $An_{43}Di_{57}$ melt viscosity due to 2.63 wt% water at 1400 °C and 1.0 GPa is 29 times of that at 1600 °C and 1.0 GPa. This is in consistent with, in $An_{43}Di_{57}$

melt, the increase of $CO_{2,t}$ diffusivity at 1400 °C and 1.0 GPa due to 2.63 wt% water (a factor of 7.2) is bigger than the increase of $CO_{2,t}$ diffusivity at 1600°C and 1.0 GPa due to the same amount of water (a factor of 1.8).

The total CO_2 diffusion data in dry and hydrous $An_{43}Di_{57}$ melts are then compared with the literature. Figure 6a shows, $CO_{2,t}$ diffusivities in dry $An_{43}Di_{57}$ melt are significantly different from the respective values predicted by the $CO_{2,t}$ diffusion model given by Equation (30) in Zhang et al. (2007) and the largest difference is 0.89 in terms of lnD. Equation (30) in Zhang et al. (2007) is valid at 550-1340 °C and the extrapolation to higher temperature may be not good, especially because the diffusion data it used are scattered a lot at the high temperature end.

Behrens and Zhang (2001) found Ar diffusivities in silicic melts are similar to total CO_2 diffusivity in all melts, which is attributed to their similarities in both molecular structure and molar mass. This phenomenon makes it possible to use Ar diffusivity to estimate $CO_{2,t}$ diffusivity. Zhang et al. (2007) reviewed Ar diffusion data in the literature and their fitting 152 Ar diffusion data in rhyolitic, dacitic, albitic and jadeitic melts at 500-1500 °C, P ≤ 1 GPa and H_2O_t ≤ 5 wt% yielded (Equation 32 in Zhang et al., 2007):

$$lnD_{Ar\ in\ silicic\ melts} = -13.99-(17367+1.9448P)/T+(855.2+0.2712P)C_w/T$$

Where C_w is weight percent of H_2O_t. Figure 6a shows, within the temperature range of the equation above, the difference between $CO_{2,t}$ diffusivity in dry $An_{43}Di_{57}$ melt and Ar diffusivity at 1.0 GPa is less than 0.2 in terms of lnD. Ar diffusivity at 1400 °C and 1.0 GPa is used for comparison instead of that at 1400 °C and 0.5 GPa is because, unlike the strong pressure dependence of Ar diffusivity, the pressure dependence of CO_2 diffusivity in dry melt can be ignored compared with temperature, which is suggested by Equation (30) in Zhang et al. (2007) and discussed with an example in the last section. On the other hand, the datum point at 1594 °C and 1.0 GPa in dry $An_{43}Di_{57}$ melt is different from Ar

diffusivity at the same condition by 1.06 in terms of lnD, which means extrapolation is not good. Thus, the Ar diffusivity model is, only exclusively in its temperature range, in consistent with the $CO_{2,t}$ diffusivity data in dry $An_{43}Di_{57}$ melt.

Figure 6b shows $CO_{2,t}$ diffusivity data in hydrous $An_{43}Di_{57}$ melt are significantly different from the respective Ar diffusivity data predicted by Equation (32) of Zhang et al. (2007), and the largest difference is 0.48 in terms of lnD. Equation (32) in Zhang et al. (2007) implied the activation energy of Ar diffusion at 1.0 GPa in hydrous melt with 2.63 wt% H_2O is 135.93 kJ·mol^{-1}, which is close to that of Equation (7), but it has a much smaller pre-exponential factor than Equation (7). The differences are due to two reasons. First, Ar diffusivities in rhyolitic, dacitic, albitic and jadeitic melts are slightly higher than those in silica melt and smaller than those in basaltic melt, likely indicating a smaller degree of polymerization contributes to a higher Ar diffusivity. Secondly and more importantly, Ar diffusivity data in hydrous melt used in fitting Equation (32) in Zhang et al. (2007) only cover a temperature range of 480-1200 °C. It may not be valid to extrapolate this equation to a much higher temperature range of 1400-1600 °C in hydrous $An_{43}Di_{57}$ melt.

Closing remarks

This study provides new total CO_2 diffusion data in both dry and hydrous $An_{43}Di_{57}$ melts. Data are fit with two Arrhenius equations: one is in dry melt and at 1.0 GPa, the other is in hydrous melt with 2.63 wt% H_2O and at 1.0 GPa. There are some outliers in the experimental diffusivity data, and the reason is not clear. It is necessary to improve the experimental data reproducibility. In the future, new experiments could be done in hydrous melts with different weight percents of H_2O to investigate more about water dependence of total CO_2 diffusivity. Inspired by figure 5, it could be also interesting to

carry out new experiments in both dry and hydrous melts at temperature higher than 1600 °C to investigate whether $CO_{2,t}$ diffusivity in dry melts will finally exceed that in hydrous melts. By constructing this new database of $CO_{2,t}$ diffusivity in hydrous melts, people can better understand how much CO_2 diffusion kinetics contributes to the degassing processes of the hydrous MORB and OIB that are oversaturated with CO_2.

Acknowledgements

Reference

Behrens, H. and Stuke, A. (2003) Quantification of H_2O contents in silicate glasses using IR spectroscopy – a calibration based on hydrous glasses analyzed by Karl-Fischer Titration. Glass Science and Technology, 76, 176-189.

Behrens, H and Zhang, Y. (2001) Ar diffusion in hydrous silicic melts: Implications for volatile diffusion mechanisms and fractionation. Earth and Planetary Science Letters, 192, 363-376.

Benne, D. and Behrens, H. (2003) Water solubility in haplobasaltic glasses. European Journal of Mineralogy, 15, 803-814.

Danyushevsky, L.V., Falloon, T.J., Sobolev, A.V., Crawford, A.J., Carroll, M., and Price, R.C. (1993) The H_2O content of basaltic glasses from southwest Pacific back-arc basins. Earth and Planetary Science Letters, 117, 347-362.

Dixon, J.E., Stolper E., and Delaney, J.R. (1988) Infrared spectroscopic measurements of CO_2 and H_2O in Juan de Fuca Ridge basaltic glasses. Earth and Planetary Science Letter, 90, 87-104.

Dixon, J.E., Stolper, E.M., Holloway, J.R. (1995) An experimental study of water and carbon dioxide solubilities in mid ocean ridge basaltic liquids. 1. Calibration and solubility models. Journal of Petrology, 36, 1607-1631.

Fine, G. and Stolper, E. (1985) The speciation of carbon dioxide in sodium alumino-Silicate glasses. Contrib. Mineral. Petrol., 91, 105-121.

Fine, G. and Stolper, E. (1986) Dissolved carbon dioxide in basaltic glasses: concentrations and speciation. Earth and Planetary Science Letters, 76, 263-278.

Hui, H. and Zhang Y. (2007) Toward a general viscosity equation for natural anhydrous and hydrous silicate melts. Geochimica et Cosmochimica Acta, 71, 403-416.

Knoche, R., Dingwell, D.B., Webb, S.L. (1992) Temperature-dependent thermal expansi-

vities of silicate melts: the system anorthite-diopside. Geochimica et Cosmochimica Acta, 56, 689–699.

Lange, R.A. (1997) A revised model for the density and thermal expansivity of K_2O-Na_2O-Cao-MgO-Al_2O_3-SiO_2 liquids from 700-1900 K: extension to crustal magmatic temperatures. Contribution to Mineralogy and Petrology, 130, 1-11.

Mungall, J.E. (2002) Empirical models relating viscosity and tracer diffusion in magmatic silicate melts. Geochimica et Cosmochimica Acta, 66, 125-143.

Nakamoto, K. (1978) Infrared and Raman Spectra of Inorganic and Coordination Compounds, 3rd edition. New York: John Wiley, 448 pp.

Ni, H., Behrens, H., and Zhang, Y. (2009) Water diffusion in dacitic melt. Geochimica et Cosmochimica Acta, 73, 3642-3655.

Nowak, M., Schreen, D., and Spickenbom, K. (2004) Argon and CO_2 on the race track in silicate melts: a tool for the development of a CO_2 speciation and diffusion model. Geochimica et Cosmochimica Acta, 68, 5127-5138.

Pandya, N., Muenow, D.W., and Sharma, S.K. (1992) The effect of bulk composition on speciation of water in submarine volcanic glasses. Geochimica et Cosmochimica Acta, 56, 1875-1883.

Presnall., D.C., Dixon, S.A., Dixon, J.R., O'Donnell, T.H., Brenner, N.L., Schrock, R.L., and Dycus, D. W. (1978) Liquids Phase Relations on the Join Diopside-Forsterite-Anorthite From 1 atm to 20 kbar: Their Bearing on the Generation and Crystallization of Basaltic Magma. Contribution to Mineralogy and Petrology, 66, 203-220.

Richet, P. and Bottinga, Y. (1984) Anorthite, andesine, wollastonite, diopside, cordierite, and pyrope: thermodynamics of melting, glass transitions, and properties of the amorphous phases. Earth and Planetary Science Letters, 67, 415-432.

Scholze, H. (1959) Der Einbau des Wssers in Glasern. Glastechnische Berichte, 32,

81-88, 142-145, 278-281.

Scholze, H. (1960) Zur Frage der Unterscheidung zwischen H_2O-Molekeln und OH-Gruppen in Glasern und Mineralen. Naturwissenschaften, 47, 226-227.

Sierralta M., Nowak, M., and Keppler, H. (2002) The influence of bulk composition on the diffusivity of carbon dioxide in Na aluminosilicate melts. American Mineralogist, 87, 1710-116.

Stolper, E.M. (1982) Water in silicate glasses: An infrared spectroscopic study. Contribution to Mineralogy and Petrology, 81, 1-17.

Taniguchi, H. (1989) Densities of melts in the system $CaMgSi_2O_6$ – $CaAl_2Si_2O_8$ at low and high pressures, and their structural significance. Contribution to Mineralogy and Petrology. 103, 325-334.

Watson, E.B., Sneeringer M.A., and Ross, A. (1982) Diffusion of dissolved carbonate in magmas: experimental results and applications. Earth and Planetary Science Letter, 61, 346-358.

Watson E.B. (1991) Diffusion of dissolved CO_2 and Cl in hydrous silicic to intermediate magmas. Geochimica et Cosmochimica Acta, 55, 1897-1902.

Workman, R.K., Hauri, E., Hart, S.R., Wang, J., and Blusztajn, J. (2006) Volatile and trace elements in basaltic glasses from Samoa: Implications for water distribution in the mantle. Earth and Planetary Science Letters, 241, 932-951.

Zarubin, D.P. (1999) Infrared spectrum of hydrogen bonded hydroxyl groups in silicate glasses. A re-interpretation. Physics and Chemistry of Glasses, 40, 184-192.

Zhang, Y. and Stolper, E.M. (1991) Water diffusion in a basaltic melt. Nature, 351, 306-309.

Zhang, Y. (1999) H_2O in rhyolitic glasses and melts: measurement, speciation, solubility, and diffusion. Reviews of Geophysics, 37, 493-516.

Zhang, Y. and Behrens, H. (2000) H_2O diffusion in rhyolitic melts and glasses. Chemical

    Geology, 169, 243-262.

Zhang, Y., Xu, Z., Zhu, M., and Wang H. (2007) Silicate melt properties and volcanic

    eruptions. Reviews of Geophysics, 45, RG4004.

Zhang, Y. and Ni, H. (2010) Diffusion of H, C, and O components in silicate melts.

    Reviews in Mineralogy and Geochemistry, 72, 175-225.

**Tabel 1** Oxides (wt%), Anorthite weight percent and density of AnDi0-AnDi5

	SiO_2	Al_2O_3	MgO	CaO	H_2O	CO_2	Total	w(An)[a]	p(g/cm3)
AnDi0	49.58	15.91	11.84	23.09	0.009	0.000	100.43	0.426	2.786
AnDi1	48.13	15.80	10.71	22.43	2.690	0.088	99.84	0.441	2.736
AnDi2	48.38	15.64	10.89	22.39	2.141	0.055	99.49	0.435	2.747
AnDi3	47.62	15.39	10.79	22.50	2.255	0.059	98.61	0.433	2.745
AnDi4	49.83	16.07	11.30	23.43	0.043	0.081	100.75	0.433	2.785
AnDi5	48.71	15.94	11.11	22.62	2.161	0.006	100.54	0.438	2.746

a: The bulk composition is roughly Anorthite-Diopside binary system, w(An) is the best fit of Anorhite weight percent.

Table 2 Experimental total CO_2 diffusivity data in haplobasaltic melts

Exp #	T(°C)	1000/T (K^{-1})	P(kbar)	duration (s)	H_2O (wt%)	$D(\mu m^2/s)$ Profile1	Profile2	Profile3	avg.	2σ/avg(%)	lnD
DifAnDi-101	1400	0.5975	5.0	3620.3	0.052	7.04	7.12	8.15	7.44	16.6	-25.62
DifAnDi-102	1456	0.5785	10.0	1826.6	0.053	25.36	23.05	30.73	26.38	29.9	-24.36
DifAnDi-103	1454	0.5790	10.0	515.2	0.036	11.46	17.15	14.46	14.36	39.7	-24.97
DifAnDi-104	1464	0.5755	10.0	274.0	0.015	12.15	17.67	15.53	15.12	36.8	-24.92
DifAnDi-106	1594	0.5355	10.0	278.2	0.061	75.13	69.44	89.48	78.02	26.5	-23.27
DifAnDi-107	1447	0.5815	10.0	213.2	2.609	219.50	203.07	173.94	198.84	23.2	-22.34
DifAnDi-108	1456	0.5784	10.0	747.8	2.656	112.64	98.98	106.01	105.88	12.9	-22.97
DifAnDi-109	1448	0.5812	10.0	72.7	2.702	79.84	91.74	77.89	83.16	18.0	-23.21
DifAnDi-110	1393	0.6001	10.0	984.4	2.591	113.51	130.49	108.34	117.45	19.7	-22.87
DifAnDi-111	1387	0.6022	10.0	263.3	2.587	48.38	50.76	36.97	45.37	32.5	-23.82
DifAnDi-112	1596	0.5349	10.0	405.5	2.650	203.85	203.11	209.26	205.41	3.3	-22.31

(1) T is the corrected interface temperature, $T=T_{exp}/(1-2.21*x^2/600)$, where T_{exp} is the experimental temperature recorded by the thermocouple, x is the distance from interface to the thermocouple tip.

(2) P is the corrected pressure, $P=P_{nom}/1.06$, where P_{nom} is the experimental nominal pressure recorded by the gauge connected to the piston-cylinder.

(3) duration is the effective duration, which is calcualted with the first method of calculating effective duration suggested by Zhang et al. (2000).

(4) H_2O is the average H_2O_t content in the diffusion couple measured after the experiment. Since H_2O diffuse orders faster than CO_2, H_2O is almost homogenous in the diffusion couple.

(5) Presnall et al. (1978) reported the melting point of $An_{40}Di_{60}$ at 7 kbar and 10kbar is 1391°C and 1417 °C, respectively. So the melting point of $An_{43}Di_{57}$ at 5kbar is less than 1391 °C. The sample was surely molten in DifAnDi101.
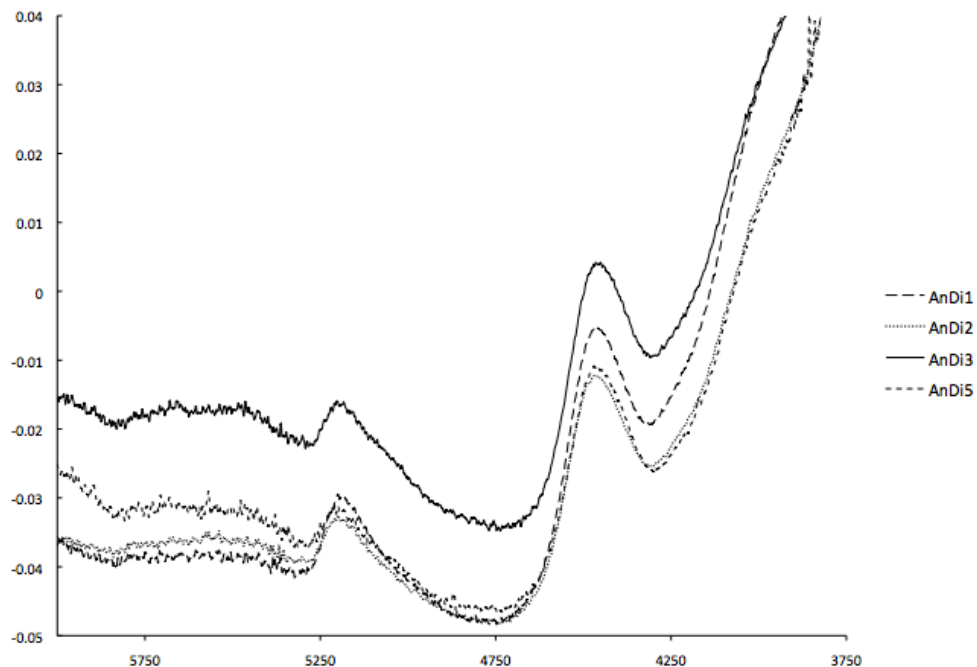
Figure 1 Background subtracted IR spectra from 6000 cm^{-1} to 3750 cm^{-1}, of AnDi1, AnDi2, AnDi3 and AnDi5, with a background of AnDi0. All the spectra have been converted based on the same sample thickness of 0.166mm.
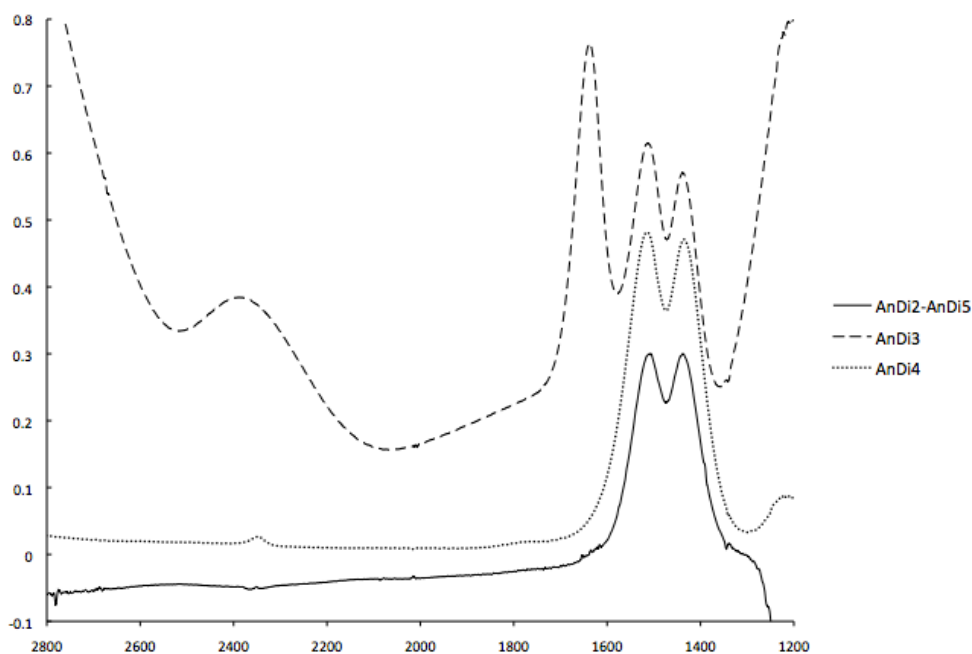
Figure 2 Background subtracted IR spectra from 2800 cm^{-1} to 1200 cm^{-1}, of AnDi3 (2.308 wt% H_2O_t, 0.0573 wt% $CO_{2,t}$) and AnDi4 (0.051 wt% H_2O_t, 0.0871 wt% $CO_{2,t}$), with a background of the dry and CO_2 free AnDi0. Background subtracted IR spectrum from 2800 cm^{-1} to 1200 cm^{-1} of AnDi2 (2.117 wt% H_2O_t, 0.0531 wt% $CO_{2,t}$) with a background of AnDi5 (2.116 wt% H_2O_t, 0.0056 wt% $CO_{2,t}$).
All the spectra have been converted based on the same sample thickness of 0.166 mm.
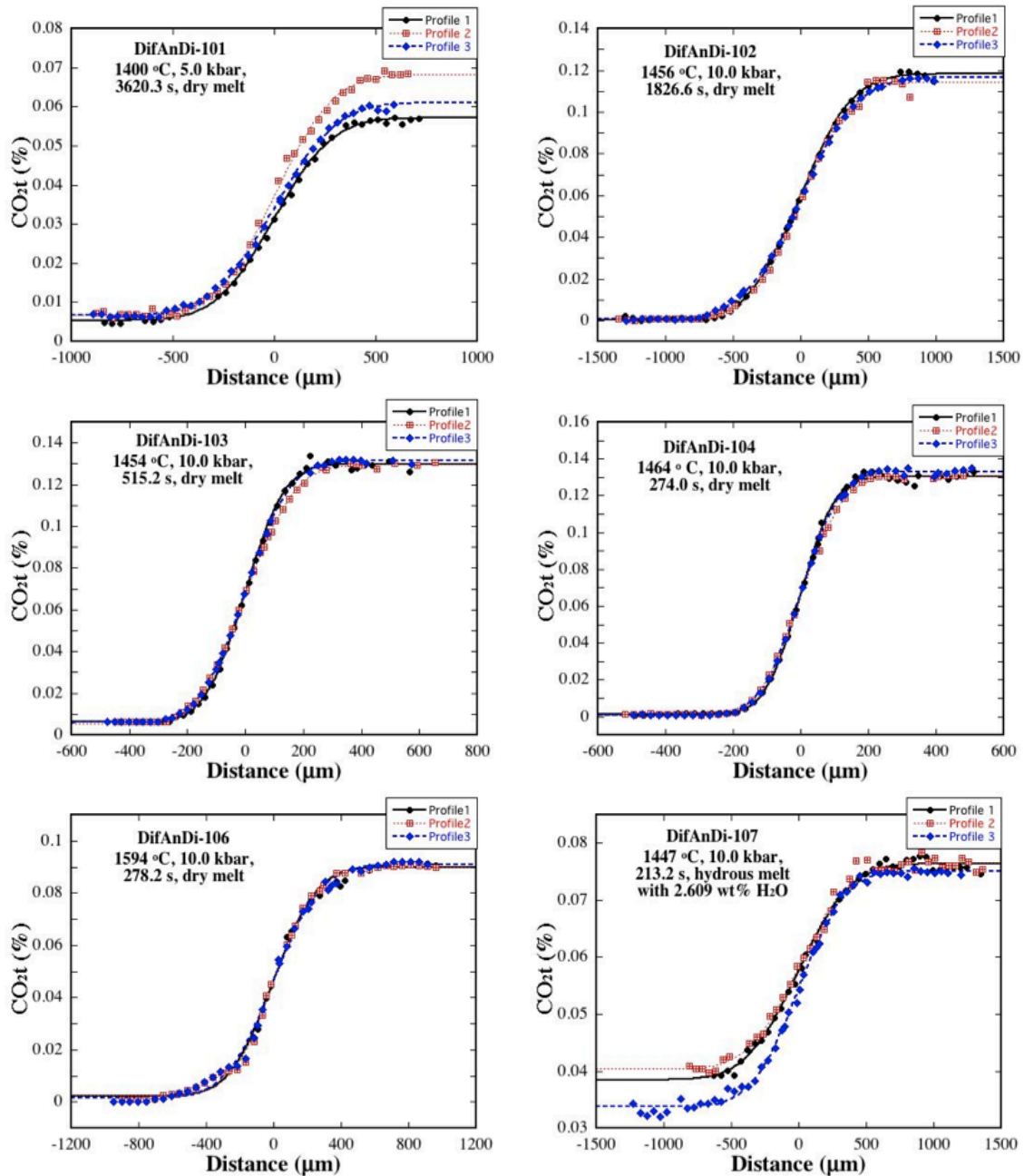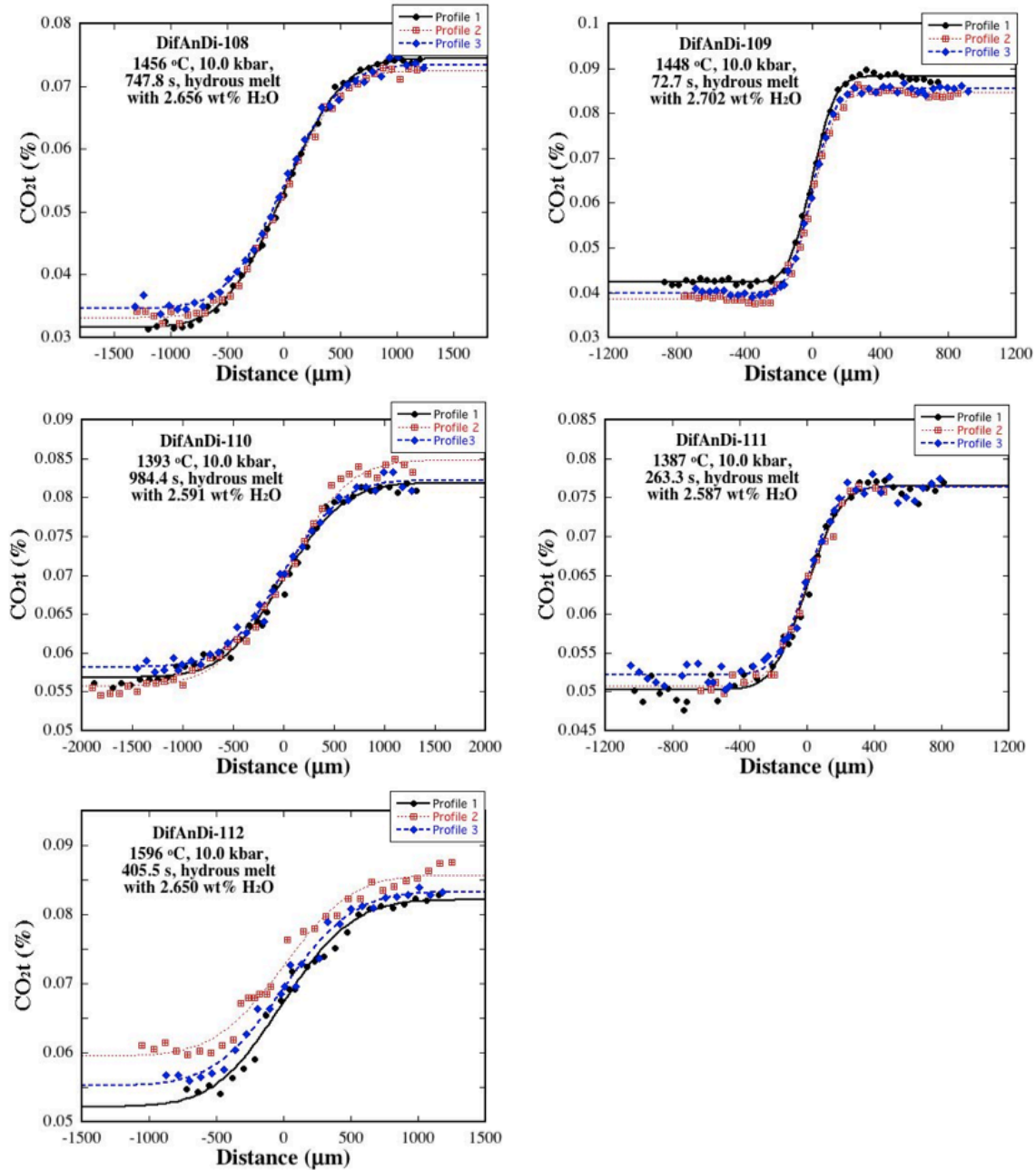* AnDi3 is moved downwards by 0.3 so that it's easier to see the three spectra together.

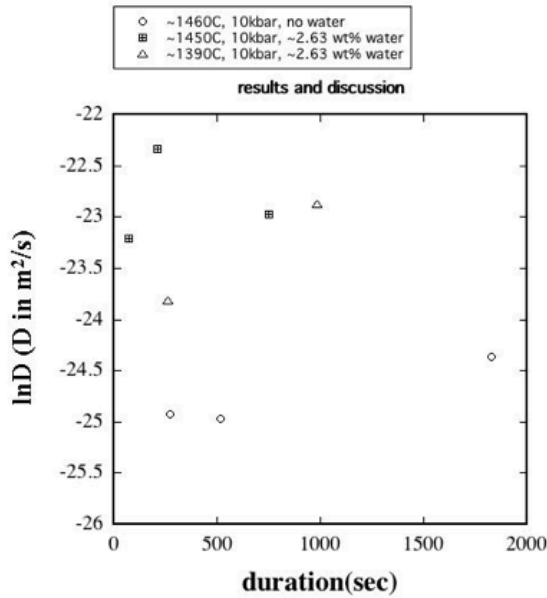Figure 3. To be continued

Figure 3 Total CO_2 content profiles in the diffusion couples. Every profile has been moved so that the interface is roughly at distance=0 μm. Every profile is fit with the analyitic solution of diffusion couple: $C=(C_R+C_L)/2+(C_R-C_L)/2*erf[x/sqrt(4Dt)]$

Figure 4 $CO_{2,t}$ diffusivity data at the same T, P and H_2O but with different durations. From the left to the right, the circles are DifAnDi-104, 103 and 102; the squares are DifAnDi-109, 107 and 108; the triangles are DifAnDi-111 and 110.
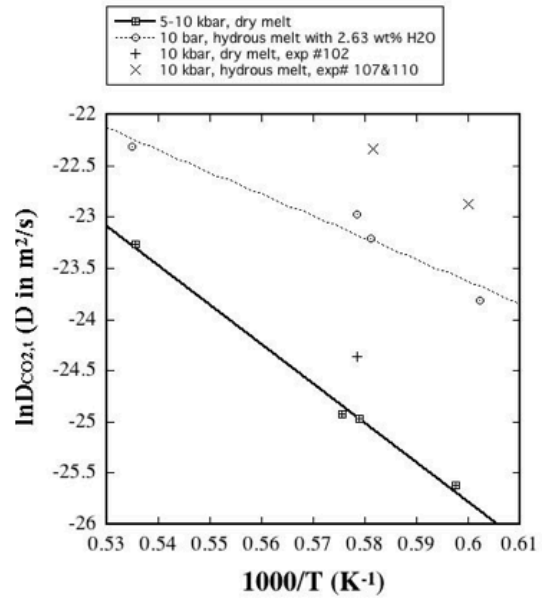
Figure 5 Experimental $CO_{2,t}$ diffusivity data in both dry and hydrous haplobasaltic glasses.
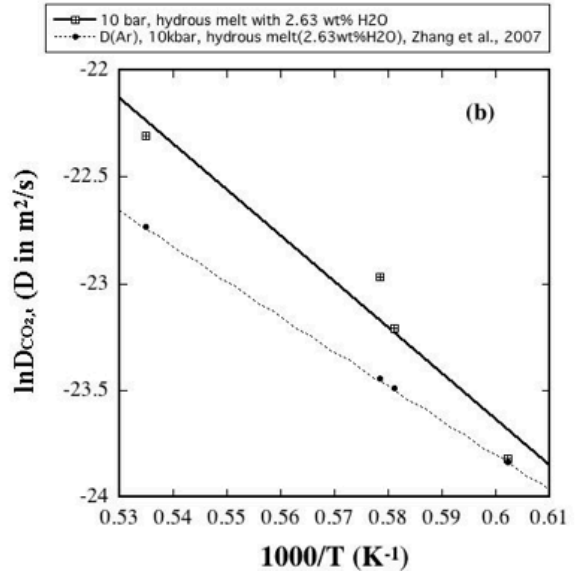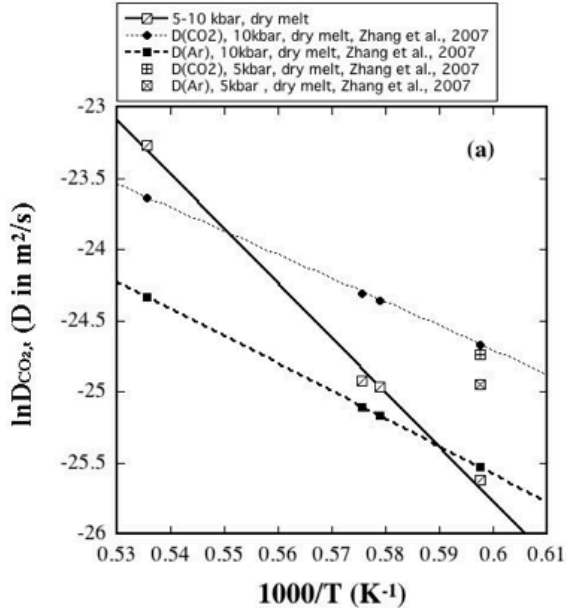
Figure 6 (a) $CO_{2,t}$ diffusion data in dry $An_{43}Di_{57}$ melt compared with $CO_{2,t}$ diffusion and Ar diffusion data in dry melts reviewed in Zhang et al. (2007).

(b) $CO_{2,t}$ diffusion data in hydrous $An_{43}Di_{57}$ melt with 2.63 wt% H_2O compared with Ar diffusion data in hydrous melt with 2.63 wt% H_2O reviewed in Zhang et al. (2007).

25